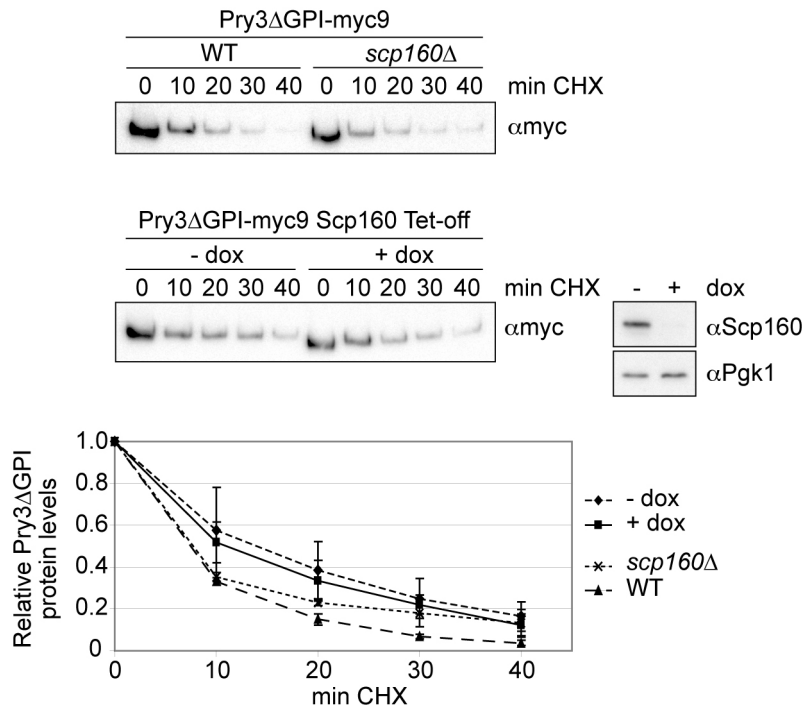
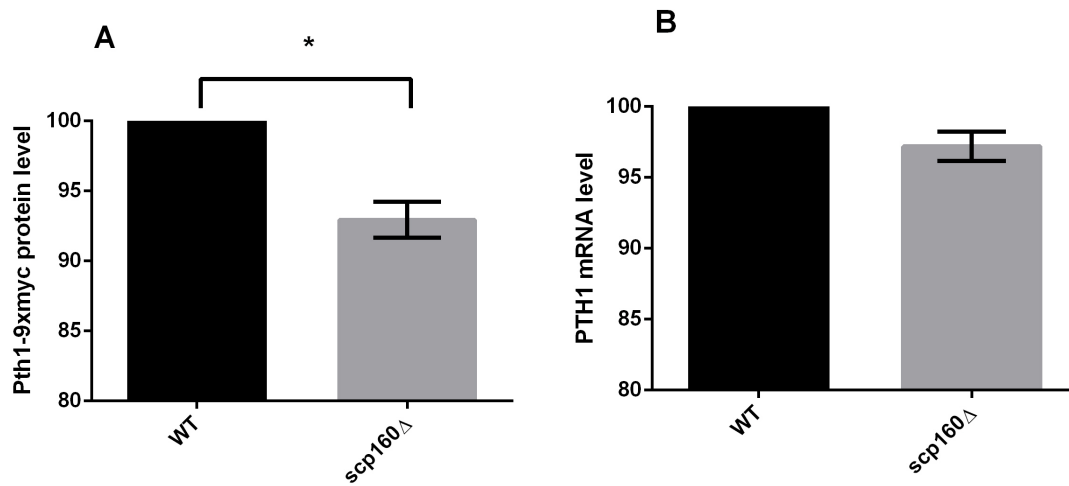


Supplementary Information (Hirschmann et al., NAR 2014)

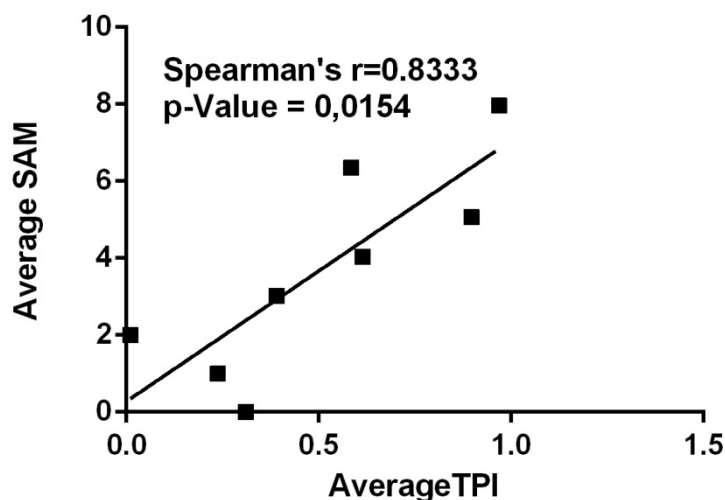
Table of contents	Page
Supplementary Figures S1-S4	2-4
Supplementary Tables S1-S8	5-12
Supplementary Methods	13-16



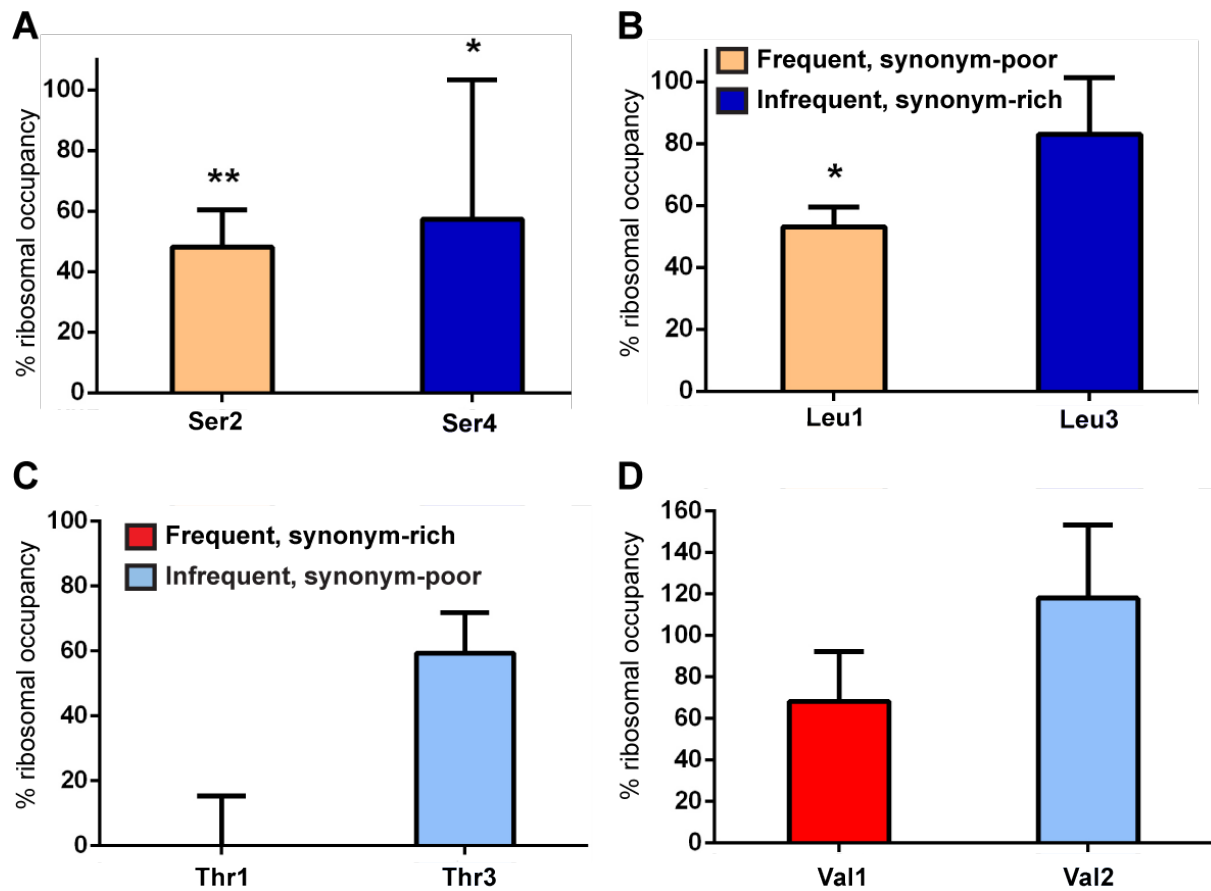
Supplementary figure S1: Stability of Pry3ΔGPI-myc9 is not affected in cells lacking Scp160p. Cycloheximide (CHX) chase analyses were performed to assess the stability of Pry3ΔGPI-myc9 in WT, *scp160Δ* and Scp160p depletion background. Logarithmically growing cultures were supplemented with 0.5 mg/ml CHX; aliquots were taken at indicated time points and immediately processed for Western blotting (see Methods section). Upper panels: Representative Western blots probed with either anti-myc antibody to detect Pry3ΔGPI-myc9 or anti-Scp160 and anti-Pgk1 antibodies to test for successful depletion of Scp160. Lower panel: Quantification of five replicates (Scp160p depletion) and three replicates (WT versus *scp160Δ*). Data are presented as mean ± standard deviation.



Supplementary figure S2. Loss of Scp160 significantly decreases Pth1 protein levels. (A) Pth1p levels in *scp160*Δ cells. Whole cell extracts were prepared from yeast cells expressing Pth1-9myc. Quantification of three independent experiments carried out. Right panel: RNA was prepared from the same strains and used for qRT-PCR. Relative *PTH1* mRNA levels are represented as the signal ratio between *scp160*Δ and WT background. All data are presented as mean ± standard deviation, n = 3. Asterisk (*) denotes significant (<0.1) p-Value for t-Test of independent behaviour between knockout and wildtype samples. (B) *PTH1* mRNA levels in *scp160*Δ cells. RNA was prepared from the same strains and used for qRT-PCR. Relative *PTH1* mRNA levels are represented as the signal ratio between *scp160*Δ and WT background. All data are presented as mean ± standard deviation, n = 2 biological replicates, analysed in technical duplicate each.



Supplementary figure S3: Average use of isoaccepting codons within subgroups of Scp160p-bound mRNAs shows pronounced nonlinear correlation with average binding reproducibility in study (1).



Supplementary figure S4: Ribosomal occupancy of tRNAs recognizing frequent codons drops more severely upon loss of eEF1a function (A, B) or after amino acid depletion (C, D). Displayed is the percentage of ribosomal occupancy (ribocc) of indicated tRNAs in *yef3(F650S)* as percentage of ribocc found in wild-type cells. The standard deviation between at least two biological replicates with two technical replicates each is indicated as bars, while * denotes p-Values <0.1 and ** denotes p-Values <0.01 for significance of independent average values between restrictive and permissive temperature levels (above columns).

(A, B): Residual ribosomal occupancy (ribocc) of tRNA pairs for amino acids serine and leucine after temperature shift of a temperature-sensitive eEF1a mutant (*yef3(F650S)*). (A) Serine, comparing Ser2 and Ser4: tRNAs recognizing only one frequent (orange) versus several infrequent (blue) codons. (B) Leucine, comparing Leu1 and Leu3: tRNAs recognizing only one frequent versus several infrequent codons.

(C, D): Residual ribosomal occupancy (ribocc) of tRNA pairs for amino acids threonine and leucine after shift from amino acid-rich (synthetic complete dextrose) to amino acid-poor (synthetic minimal dextrose) media. (C) Threonine, comparing Thr1 and Thr3: tRNAs recognizing several frequent (red) versus only one infrequent (light blue) codon. (D) Valine, comparing Val1 and Val2: tRNAs recognizing several frequent versus only one infrequent codon.

Supplementary table S1: Plasmids used in this study.

Number	Name	Short description	Source
pRJ148	pRS316		(2)
pRJ957	pCM182		(3)
pRJ1220	pYM18	9xmyc	(4)
pRJ1464	pMS342	<i>SCP160</i> ORF	(5)
pRJ1463	pCM182- <i>SCP160</i>	Tet _{off} - <i>SCP160</i>	this study
pRJ1845	pTKB595	<i>pyef3(F650S)</i>	(6)
pHS4	pRS316- <i>SCP160</i>		this study
pHS9	pRS316- <i>SCP160myc9</i>	Expression of myc9-tagged Scp160	this study
pHS10	pRS316- <i>scp160ΔKH13/14-myc9</i>	Expression of myc9-tagged Scp160 lacking KH domains 13 and 14	this study

Supplementary table S2: Yeast strains used in this study.

Strain	Relevant genotype	Plasmid	Source
W303a	<i>MATa ade2-1 trp1-1 can1-100 leu2-3,112 his3-11,15 ura3</i>	-	
RJY497	<i>scp160Δ::kITRP1</i>	-	this study
RJY3178	<i>scp160Δ::HIS3MX6</i>	-	this study
RJY3180	<i>scp160Δ::HIS3MX6 Tet_{off}-SCP160</i>	pRJ1463	this study
RJY3509	<i>SCP160-myc9::kITRP1</i>	-	this study
RJY3512	<i>SHE2-myc9::kITRP1</i>	-	this study
RJY3652	<i>CCW14-myc9::KanMX6</i>	-	this study
RJY3676	<i>CCW14-myc9::KanMX6 scp160Δ::HIS3MX6</i>	pRJ1463	this study
RJY3677	<i>CCW14-myc9::KanMX6 scp160Δ::HIS3MX6</i>	-	this study
RJY3687	<i>RPL16a-TEV-ProtA::HIS3MX6</i>	-	this study
RJY3688	<i>RPL16a-TEV-ProtA::KanMX6</i>	-	this study
RJY3689	<i>scp160Δ::kITRP1 RPL16a-TEV-ProtA::HIS3MX6</i>	-	this study
RJY4275	<i>yef3Δ::KanMX6 pyef3(F650S)</i>	pRJ1845	this study
RJY4282	<i>scp160Δ::HIS3MX6 Tet_{off}-SCP160 RPL16a-TEV-ProtA::KanMX6</i>	pRJ 1463	this study
RJY4288	<i>yef3Δ::KanMX6 pyef3(F650S) RPL16a-TEV-ProtA::HIS3MX6</i>	pRJ1845	this study
RJY4478	<i>PTH1-myc9::KanMX6</i>	-	this study
RJY4481	<i>PTH1-myc9::KanMX6 scp160Δ::kITRP1</i>	-	this study
HSY11	<i>scp160Δ::HIS3MX6 pRS316-SCP160myc9</i>	pHS9	this study
HSY12	<i>scp160Δ::HIS3MX6 pRS316-SCP160ΔKH13/14-myc9</i>	pHS10	this study
HSY15	<i>KHD1-myc9::kITRP1</i>	-	this study
HSY19	<i>PRY3ΔGPI-myc9::KanMX6</i>	-	this study
HSY20	<i>PRY3ΔGPI-myc9::KanMX6 scp160Δ::HIS3MX6</i>	-	this study
HSY21	<i>PRY3ΔGPI-myc9::KanMX6 scp160Δ::HIS3MX6 Tet_{off}-SCP160</i>	pRJ 1463	this study

All strains are derived from W303a (*MATa ade2-1 trp1-1 can1-100 leu2-3,112 his3-11,15 ura3*).

Supplementary table S3: Oligonucleotides used in this study.

In the following list, only oligos used for plasmid generation, site-directed mutagenesis and RT-qPCR are listed. Oligos used for gene knock-outs, taggings and checking of transformants were generated according to standard protocols (4, 7).

Number	Name	Sequence	Purpose
RJO2583	Scp160BamHI FW	CGCAAAGGATCCATGTCTGAAGAACAAACCGC	subcloning
RJO2584	Scp160PstI RV	CGCAAAGGATCCATGTCTGAAGAACAAACCGC	subcloning
RJO2920	ACT1 FW	TCAGAGCCCCAGAAGCTTTG	RT-qPCR
RJO2921	ACT1 RV	TTGGTCAATACCGGCAGATTC	RT-qPCR
RJO3188	CFT1 FW	TTGGCCAACGACTTTTATCAGA	RT-qPCR
RJO3189	CFT1 RV	CGCAATGCTTTTCCGTCTATC	RT-qPCR
RJO3198	PRY3 FW	CAAACGAAGGCACCTCTTCC	RT-qPCR
RJO3199	PRY3 RV	TTGCACCTAGGCTTGTGCTG	RT-qPCR
RJO3332	CCW14 FW	CAAGGCTTCTCCACCGAAT	RT-qPCR
RJO3333	CCW14 RV	GGAAGCTTGCTGCTCGAAG	RT-qPCR
RJO3373	PTH1 FW	AACCACACCCACCTCAAACC	RT-qPCR
RJO3374	PTH1 RV	TAAAACCGTGGCCGTTGG	RT-qPCR
RJO4324	Ser4 FW	ATTCCTCAGAAAAGCAATTA	RT-qPCR
RJO4325	Ser4 RV	CGTCACAGACAGGATTC	RT-qPCR
RJO4340	Ser2 FW	GGCACTATGGCCGAGT	RT-qPCR
RJO4341	Ser2 RV	CGACACCAGCAGGATTT	RT-qPCR
RJO4336	Leu1 FW	GGAGGGTTGGCCGAGT	RT-qPCR
RJO4337	Leu1 RV	CGCGGACAACCGTCCA	RT-qPCR
RJO4338	Leu3 FW	GGTACTCTGGCCGAGT	RT-qPCR
RJO4339	Leu3 RV	CGCGCCTCCGAAGAGA	RT-qPCR
RJO4393	Thr1 FW	GCCAAGTTGGTAAGGCGCCAC	RT-qPCR
RJO4394	Thr1 RV	CGGATTTGAACCGATGATCT	RT-qPCR
RJO4397	Thr3 FW	GCCAAGTGGTAAGGCATCGCA	RT-qPCR
RJO4398	Thr3 RV	GGGAATTGAACCCACGATCC	RT-qPCR
RJO4399	Val1 FW	GTCTAGTCGGTTATGGCATCT	RT-qPCR
RJO4400	Val1 RV	ATCGAACTGGGGACGTTCTG	RT-qPCR
RJO4401	Val2 FW	GTGTAGCGGCTATCACGTTGC	RT-qPCR
RJO4402	Val2 RV	GATCGAACTCGGGACCTTTG	RT-qPCR

Supplementary table S4: TSC (Translational State Change), reflecting shift of mRNAs towards sucrose gradient fractions of higher density (polysomes) following SCP160 depletion.

ORF	Gene	TSC depleted/control ^a	Polysomal RNA depleted/control ^b	Monosomal RNA depleted/control ^c	Total RNA depleted/control ^d
YPR159C-A	---	3.7	1.4	-2.3	1.0
YHR213W	---	2.7	1.9	-1.3	1.1
YJL078C*	PRY3*	2.7*	2.1*	-1.3*	-1.0*
YCR089W	FIG2	2.6	1.8	-1.3	1.4
YLR139C	SLS1	2.6	2.1	-1.2	1.4
YAL065C	---	2.6	1.6	-1.5	1.1
YJR151C	DAN4	2.4	1.7	-1.3	-1.0
YNR044W*	AGA1*	2.4*	2.2*	-1.1*	1.4*
YHR189W	PTH1	2.4	1.7	-1.3	1.0
YCL021W-A	---	2.3	1.9	-1.1	1.2
YDR420W	HKR1	2.2	2.2	-1.0	1.1
YIR019C	<i>MUC1</i>	2.2	1.7	-1.2	1.0
YPL085W	SEC16	2.2	1.6	-1.3	1.2
YLR337C	VRP1	2.2	1.8	-1.1	-1.1
YNL271C	<i>BNI1</i>	2.2	1.7	-1.2	1.1
YLR013W	<i>GAT3</i>	2.2	1.4	-1.4	1.0
YMR175W-A	---	2.1	1.4	-1.5	1.0
YAR050W	<i>FLO1</i>	2.1	1.6	-1.3	1.0
YAR009C	---	2.1	2.3	1.1	-1.1
YJL216C	---	2.1	1.3	-1.5	1.4
YKR102W	FLO10	2.0	1.5	-1.3	1.2
YOR181W	<i>LAS17</i>	2.0	1.5	-1.3	1.0
YBL074C	<i>AAR2</i>	2.0	1.5	-1.3	1.2
YOL019W-A	---	2.0	1.1	-1.7	1.0
YMR070W	<i>MOT3</i>	2.0	1.7	-1.1	1.5
YLR315W	NKP2	2.0	1.2	-1.7	-1.2
YOR316C-A	---	1.9	1.3	-1.5	1.1
YBR072C-A	---	1.9	1.2	-1.7	1.0
YNL277W-A	---	1.9	1.1	-1.7	-1.3
YNL068C	<i>FKH2</i>	1.9	1.6	-1.1	1.0
YCR108C	---	1.9	1.2	-1.6	-1.0
YDL039C	<i>PRM7</i>	1.9	1.7	-1.1	2.4
YCR068W	<i>ATG15</i>	1.9	1.6	-1.1	-1.0
YER132C	<i>PMD1</i>	1.9	1.5	-1.2	1.1
YGR023W	<i>MTL1</i>	1.9	1.9	1.0	-1.8
YBL044W	---	1.9	1.1	-1.8	1.1
YNL093W	<i>YPT53</i>	1.9	1.0	-1.7	-2.0
YEL035C	<i>UTR5</i>	1.9	1.3	-1.4	1.1
YLR390W-A*	CCW14*	1.8*	-1.0*	-1.8*	1.0*
YNL034W	---	1.8	1.3	-1.4	1.3
YLR393W	<i>ATP10</i>	1.8	1.2	-1.5	1.1
YDL195W	<i>SEC31</i>	1.8	1.3	-1.3	1.0
YEL019C	<i>MMS21</i>	1.8	1.2	-1.6	-1.0
YLR136C	<i>TIS11</i>	1.8	1.3	-1.4	-1.8
YOR394C-A	---	1.8	1.5	-1.2	1.2
YOR329C	<i>SCD5</i>	1.8	1.4	-1.2	-1.0
YGR014W*	MSB2*	1.8*	1.7*	-1.0*	1.1*
YGR249W	<i>MGA1</i>	1.8	1.4	-1.5	-3.9
YDR034C-A	---	-1.8	-2.1	-1.6	1.2
YGR109W-A	---	-1.8	-1.4	1.1	1.2
YDL156W	---	-1.8	-1.2	1.2	-1.0
YFL024C	<i>EPL1</i>	-1.9	1.1	1.6	1.1
YFL068W	---	-1.9	-1.6	1.1	1.1
YER014C-A	<i>BUD25</i>	-1.9	-1.9	-1.3	1.1
YIR018C-A	---	-2.0	-2.1	-1.4	1.1
YGL168W	HUR1	-2.1	-2.2	-1.2	1.2
YFR035C	---	-2.1	-2.4	-1.6	1.0
YGR240C-A	---	-2.2	-2.2	-1.4	1.3
YGR035W-A	---	-2.2	-2.0	-1.1	1.9
YDR524W-A	---	-2.8	-3.2	-2.0	1.4

mRNAs tested by IP-qRT-PCR are in bold; mRNAs associated with Scp160 are marked with an asterisk.

^a Changes in translation state (heavy/light (D) / heavy/light (C))

^c Changes in monosomal and mRNP associated mRNA pool

^b Changes in polysomal mRNA pool

^d Changes in total mRNA pool

Supplementary table S5: Candidate mRNAs from (1) with varying extent of reproducible Scp160p binding, as indicated via ordering by falling significance analysis of microarray (SAM) binding scores.

Gene	ORF	SAM threshold	Gene	ORF	SAM threshold
<i>AGA1</i>	<i>YNR044W</i>	8	<i>DOA1</i>	<i>YKL213C</i>	3
<i>BMS1</i>	<i>YPL217C</i>	7	<i>GOR1</i>	<i>YNL274C</i>	3
<i>SPF1</i>	<i>YEL013W</i>	7	<i>TOM70</i>	<i>YNL121C</i>	3
<i>PMT4</i>	<i>YJR143C</i>	7	<i>SLA1</i>	<i>YBL007C</i>	3
<i>UTP10</i>	<i>YJL109C</i>	7	<i>TRM10</i>	<i>YOL093W</i>	3
<i>ERG4</i>	<i>YGL012W</i>	7	<i>CRN1</i>	<i>YLR429W</i>	3
<i>FUS3</i>	<i>YBL016W</i>	6	<i>ILV1</i>	<i>YER086W</i>	3
<i>CRH1</i>	<i>YGR189C</i>	6	<i>SEC31</i>	<i>YDL195W</i>	3
<i>SCP160</i>	<i>YJL080C</i>	6	<i>CSI2</i>	<i>YOL007C</i>	3
<i>FAS1</i>	<i>YKL182W</i>	6	<i>CCW14</i>	<i>YLR390W-A</i>	3
<i>PRP19</i>	<i>YLL036C</i>	6	<i>MSB2</i>	<i>YGR014W</i>	3
<i>LSG1</i>	<i>YGL099W</i>	6	<i>POM34</i>	<i>YLR018C</i>	3
<i>SVL3</i>	<i>YPL032C</i>	6	<i>MRPL3</i>	<i>YMR024W</i>	2
<i>IMH1</i>	<i>YLR309C</i>	6	<i>PMD1</i>	<i>YER132C</i>	2
<i>NGR1</i>	<i>YBR212W</i>	6	-	<i>YPL260W</i>	2
<i>FEN1</i>	<i>YCR034W</i>	6	<i>LTV1</i>	<i>YKL143W</i>	2
<i>FKS1</i>	<i>YLR342W</i>	6	<i>LPX1</i>	<i>YOR084W</i>	2
<i>ROX1</i>	<i>YPR065W</i>	6	<i>DNM1</i>	<i>YLL001W</i>	2
<i>GNP1</i>	<i>YDR508C</i>	6	<i>DHR2</i>	<i>YKL078W</i>	2
<i>CDC48</i>	<i>YDL126C</i>	5	<i>TYS1</i>	<i>YGR185C</i>	2
<i>RPG1</i>	<i>YBR079C</i>	5	<i>MRP4</i>	<i>YHL004W</i>	2
-	<i>YJR015W</i>	5	<i>GRC3</i>	<i>YLL035W</i>	2
<i>KAP123</i>	<i>YER110C</i>	5	<i>PDX1</i>	<i>YGR193C</i>	1
<i>ILS1</i>	<i>YBL076C</i>	5	<i>PDA1</i>	<i>YER178W</i>	1
<i>HNM1</i>	<i>YGL077C</i>	5	-	<i>YFL042C</i>	1
<i>STO1</i>	<i>YMR125W</i>	5	<i>PXL1</i>	<i>YKR090W</i>	1
<i>ALO1</i>	<i>YML086C</i>	5	<i>MUD2</i>	<i>YKL074C</i>	1
<i>SED1</i>	<i>YDR077W</i>	5	<i>DUR1,2</i>	<i>YBR208C</i>	0
<i>NCP1</i>	<i>YHR042W</i>	5	<i>ULA1</i>	<i>YPL003W</i>	0
<i>PMT3</i>	<i>YOR321W</i>	4	<i>GRX3</i>	<i>YDR098C</i>	0
<i>ELP3</i>	<i>YPL086C</i>	4	<i>RPS11A</i>	<i>YDR025W</i>	0
<i>ASN2</i>	<i>YGR124W</i>	4	<i>RER1</i>	<i>YCL001W</i>	0
<i>MPT5</i>	<i>YGL178W</i>	4			
<i>KEM1</i>	<i>YGL173C</i>	4			
- (<i>eIF2A</i>)	<i>YGR054W</i>	4			
<i>SPT6</i>	<i>YGR116W</i>	4			
<i>CHA1</i>	<i>YCL064C</i>	4			
<i>RPD3</i>	<i>YNL330C</i>	4			
<i>SRP68</i>	<i>YPL243W</i>	4			
<i>PRY3</i>	<i>YJL078C</i>	4			
<i>APL6</i>	<i>YGR261C</i>	3			

Supplementary table S6: Average TPI (codon autocorrelation) and SAM (Scp160p binding reproducibility) within subgroups from (1) study. P-values indicate significance of independent average values from neighboring subgroups.

TPI	SAM	p-Value
0,96876	7,96225395	0,01232367
0,58443562	6,34962134	6,11E-14
0,89711	5,05912218	1,01E-16
0,61362	4,03717479	5,62E-24
0,39075	3,01952924	1,95E-19
0,0102	2,00496162	2,68E-31
0,2381	0,99863794	7,98E-21

Supplementary table S7: Candidate mRNAs from Supplementary Table S4 with varying extent of translational depletion following Scp160p depletion, as indicated via ordering by falling translational state change (TSC) values.

Gene	ORF	TSC	Gene	ORF	TSC
	YPR159C-A	3,71	<i>MMS21</i>	YEL019C	1,82
	YHR213W	2,67	<i>TIS11</i>	YLR136C	1,82
<i>PRY3</i>	YJL078C	2,66	<i>MSB2</i>	YGR014W	1,81
<i>FIG2</i>	YCR089W	2,6		YOR394C-A	1,81
<i>SLS1</i>	YLR139C	2,6	<i>SCD5</i>	YOR329C	1,81
	YAL065C	2,59	<i>MGA1</i>	YGR249W	1,8
<i>DAN4</i>	YJR151C	2,42		YDR034C-A	0,55
<i>PTH1</i>	YHR189W	2,4		YGR109W-A	0,55
	YAL065C	2,29		YDL156W	0,55
<i>HKR1</i>	YDR420W	2,23	<i>EPL1</i>	YFL024C	0,52
<i>MUC1</i>	YIR019C	2,21		YFL068W	0,52
<i>SEC16</i>	YPL085W	2,18	<i>BUD25</i>	YER014C-A	0,52
<i>AGA1</i>	YNR044W	2,17		YIRO18C-A	0,51
<i>VRP1</i>	YLR337C	2,17	<i>HUR1</i>	YGL168W	0,47
<i>BNI1</i>	YNL271C	2,17		YFR035C	0,47
<i>GAT3</i>	YLR013W	2,15		YGR240C-A	0,46
<i>FLO1</i>	YAR050W	2,09		YGR035W-A	0,45
	YAR009C	2,07		YDR524W-A	0,36
<i>FLO10</i>	YKR102W	2,05	<i>CFT1</i>	YDR301W	0
	YJL216C	2,05	<i>POM34</i>	YLR018C	-
<i>LAS17</i>	YOR181W	2,01			
<i>AAR2</i>	YBL074C	2,01			
	YOL019W-A	2			
<i>MOT3</i>	YOL019W-A	1,97			
<i>NKP2</i>	YLR315W	1,95			
	YOR316C-A	1,95			
	YBR072C-A	1,94			
	YNL277W-A	1,94			
<i>FKH2</i>	YNL068C	1,91			
	YCR108C	1,91			
<i>ATG15</i>	YCR068W	1,9			
<i>PRM7</i>	YDL039C	1,9			
<i>PMD1</i>	YER132C	1,89			
<i>MTL1</i>	YGR023W	1,88			
	YBL044W	1,87			
<i>YPT53</i>	YNL093W	1,87			
<i>UTR5</i>	YEL035C	1,85			
<i>CCW14</i>	YLR390W-A	1,84			
	YNL034W	1,84			
<i>ATP10</i>	YLR393W	1,83			
<i>SEC31</i>	YDL195W	1,83			

Supplementary table S8: Average TPI for individual amino acids (= codon autocorrelation at amino acid level), in mRNA target subgroups ordered by TSC (degree of mRNA distribution shift in polysome gradients) threshold, from figure 5. P-values indicate significance by comparison with 100,000 random genomic pickings of equally sized groups. TPI was calculated for the whole set respectively, up to the indicated TSC threshold.

TSC threshold	Serine		Leucine	
	TPI	p-Val	TPI	p-Val
0.3	0.116	0.277	0.175	0.397
0.5	0.132	0.343	0.166	0.433
1.8	0.0830	0.187	0.122	0.378
2.0	0.128	0.374	0.124	0.413
2.2	0.441	0.067	0.204	0.388
2.4	0.598	0.018	0.276	0.283
2.6	0.535	0.089	0.181	0.464

TSC threshold	Threonine		Valine	
	TPI	p-Val	TPI	p-Val
0.3	0.293	0.00418	0.0546	0.403
0.5	0.319	0.00189	0.0567	0.394
1.8	0.324	0.00248	0.0560	0.405
2.0	0.576	0.00002	0.180	0.133
2.2	0.652	0.00043	0.103	0.353
2.4	0.600	0.00490	0.177	0.258
2.6	0.573	0.02880	0.301	0.174

Supplementary Methods

Standard Methods

Many of the following microbiological and biochemical, as well as molecular biological methods such as restriction digests, dephosphorylation of fragments, ligations and separation of DNA in agarose gels are based on standard techniques (8, 9). Commercially available kits were used according to the manufacturer's instructions. Plasmids were sequenced by Eurofins MWG Operon (www.eurofinsdna.com). For all methods described, deionised water was used unless RNA isolation was concerned, where DEPC-treated/ HPLC-grade deionized water was used.

Plasmids

Plasmids used or generated during this study are listed in **Supplementary table S1**. The centromeric plasmid pCM182 (3) was used to clone *SCP160* under the control of the repressible tetracycline operator. The *SCP160* ORF was amplified by PCR from vector pMS342 (gift from M. Seedorf) and cloned as BamHI-PstI fragment into pCM182. The resulting plasmid RJP1463 was sequenced and confirmed by FACS analysis to complement an *scp160* deletion.

For the generation of plasmids carrying tagged *SCP160* versions, 681 bp of the *SCP160* promoter region and the first 1836 bp of the *SCP160* ORF were amplified as well as a fragment spanning the last 1783 nt of the *SCP160* ORF and 286 nt of the *SCP160* terminator. These PCR products were cloned into plasmid pRS426 (2). Plasmid HSP4 was produced from this by subcloning the complete *SCP160* gene into pRS316 (2) using BamHI/SalI. The insertion of the myc9 tag into HSP4 to generate HSP9 was done as follows. First, the myc9 nucleotide sequence flanked by BglII restriction sites was amplified from plasmid pYM19 (4). The stop codon of *SCP160* in HSP4 was changed to a BglII site by site-directed mutagenesis. The myc9 fragment was inserted in frame after the *SCP160* ORF and the correct orientation of the insert was confirmed.

Pry3p overexpression constructs were generated as follows. To create HSP12, the *GAL1* promoter of plasmid p415GAL1 (10) was replaced by the constitutively active *GPD1* promoter of pYM-N14 (4). Then, the *PRY3* ORF obtained from genomic DNA by PCR with was introduced using the HindIII site, resulting in plasmid HSP11.

Yeast strains

All strains (**Supplementary table S2**) are derived from haploid (*MATa*) or diploid (*MATa/MATa*) W303 background (*ade2-1 trp1-1 can1-100 leu2-3,112 his3-11,15 ura3-52*).

The chromosomal deletion of yeast genes as well as the C- or N-terminal insertion of epitope tags were performed by a PCR-based strategy (4, 7). Transformants were analyzed for correct integration of the module by colony PCR; epitopetagging was in addition confirmed by Western Blot analysis of whole cell extracts.

To generate a truncated version of Pry3p lacking the GPI modification site (Pry3ΔGPI_{myc9}), oligonucleotides were designed to insert the tag 90 base pairs upstream of the *PRY3* stop codon.

Strain RJY3180, expressing Scp160p under control of a repressible Tet operator, was generated as follows. In diploid a W303 strain, one copy of the *SCP160* ORF was deleted, resulting in a heterozygous strain *SCP160/scp160::HIS3MX6*, into which plasmid RJP1463 (carrying *SCP160* under control of the Tet operator) was introduced. After sporulation, clones were identified that carried the *scp160* deletion and plasmid RJP1463. FACS analysis demonstrated that RJP1463 functionally complements the *scp160* deletion. Depletion of Scp160p in strain RJY3180 and all strains derived from it was induced by addition of 2 µg/ml doxycycline to the culture medium.

Strains expressing *SCP160* variants from centromeric plasmids were created by introducing the respective plasmid into a *SCP160/scp160::HIS3MX6* strain, subsequent sporulation, and tetrad dissection.

Preparation of whole cell extracts for immunoblotting

15-20 OD_{600nm} units of cells were harvested, resuspended in 1 ml of lysis buffer (20 mM Hepes-KOH pH 7.6, 100 mM potassium acetate, 5 mM magnesium acetate, 1 mM EDTA, 2 mM DTT, 0.5 mM PMSF and 0.25 mM benzamidine) and vortexed for 5 min with 400 µl of glass beads. After centrifugation (2 min, 100 × g), the supernatant was collected, sample loading buffer was added and samples were incubated at 65°C for 10 min. Scp160p was detected by a specific antibody (5). Phosphoglycerokinase (P_{gk1p}), actin (Act_{1p}) and the HA epitope were detected by commercially available antibodies. Signals were detected with an LAS-3000 mini system (Fujifilm) equipped with a CCD camera. Image processing and signal quantification was performed with Image Reader and Multi Gauge softwares (Fujifilm).

Flow cytometry

Samples for FACS analysis were prepared as described (12) and analyzed in a FACS Calibur™ flow cytometer (Becton Dickinson). Propidium iodide fluorescence was detected in

the FL2 channel (585/42 nm). Data were collected using CellQuest™ software (Becton Dickinson) and analyzed with WinMDI version 2.8, provided by Joseph Trotter (Scripps Research Institute, La Jolla, CA).

Sample preparation for microarray hybridization

20 OD_{600nm} units of logarithmically growing cells were harvested and resuspended in 500 µl Cross RNA buffer I (0.3 M NaCl, 10 mM Tris/HCl pH 7.5, 1 mM EDTA, 0.2% SDS). 200 µl of glass beads and 400 µl of phenol/chloroform/isoamyl alcohol (25:24:1) were added and the samples were vortexed for 10 min. After centrifugation, RNA was precipitated from the aqueous phase with ethanol. DNase treatment and reverse transcription were carried out as described above. For microarray analysis samples, a spin-column based method (NucleoSpin RNA Clean-Up, Macherey-Nagel) was applied according to the manufacturer's specifications in order to purify the DNase-treated RNA.

All subsequent steps were conducted by the Kompetenzzentrum für Fluoreszenz Bioanalytik, Regensburg (<http://www.kfb-regensburg.de>). Quality and quantity of the RNA were determined using an Agilent 2100 bioanalyzer (Agilent Technologies). For the preparation of biotinylated probes, the MessageAmp II Biotin Enhanced Kit (Ambion) was used. Biological sample duplicates were hybridized to Affymetrix Yeast Genome 2.0 Arrays.

Microarray handling and data analysis

Raw signal intensities for each probe in the .CEL files were analyzed using version 6.4 of the PARTEK GENOMICS SUITE software (Partek Inc.). Data were filtered by application of an expanded mask file that was based on the *s_cerevisiae.msk* file of Affymetrix, to mask the *S. pombe* probe sets, unspecific probe sets, and replicate probe sets of *S. cerevisiae*. The robust multiarray average (RMA) normalization method was used for background correction (11), quantile normalization and medianpolish probe set summarization. Since the arrays were scanned on different days, a principal component analysis (PCA) revealed a batch effect. This effect was removed by the batch effect removal tool implemented in the PARTEK software package. In a first step, the translational state (= mRNA abundance in heavy versus light fractions) was calculated for all mRNAs in control and Scp160p depleted cells. This was done with one-way analysis of variance (ANOVA) applying a linear contrast to compare heavy (“H”) with baseline light (“L”) samples. In a second step, the translational state change was calculated for all mRNAs as follows: $(H_{\text{dox}}/L_{\text{dox}}) / (H_{\text{wt}}/L_{\text{wt}})$. The translational state of mRNAs of Scp160p depleted cells were compared to baseline control cells. Genes listed as “dubious open reading frames (ORFs)” in the Saccharomyces Genome Database (SGD) were removed. The final gene list was further filtered by a translational state change cut-off value of ≥ 1.8 or

≤ -1.8 in order to reveal mRNAs with stronger shifts in their efficiency of translation. Microarray data were deposited in the ArrayExpress data base with accession number E-MEXP-2581.

For systematic classification of significantly over-represented biological processes and subcellular localizations, the list of genes with significant translational state changes (cut-off value of ≥ 1.8 or ≤ -1.8) was analyzed on the basis of the MIPS Functional Catalogue Database (FunCatDB). Only over-represented terms with a p-value < 0.01 were considered.

References

1. Hogan,D.J., Riordan,D.P., Gerber,A.P., Herschlag,D. and Brown,P.O. (2008) Diverse RNA-binding proteins interact with functionally related sets of RNAs, suggesting an extensive regulatory system. *PLoS Biol*, **6**, e255.
2. Sikorski,R.S. and Hieter,P. (1989) A system of shuttle vectors and yeast host strains designed for efficient manipulation of DNA in *Saccharomyces cerevisiae*. *Genetics*, **122**, 19–27.
3. Belli,G., Garí,E., Piedrafita,L., Aldea,M. and Herrero,E. (1998) An activator/repressor dual system allows tight tetracycline-regulated gene expression in budding yeast. *Nucleic Acids Res*, **26**, 942–947.
4. Janke,C., Magiera,M.M., Rathfelder,N., Taxis,C., Reber,S., Maekawa,H., Moreno-Borchart,A., Doenges,G., Schwob,E., Schiebel,E., et al. (2004) A versatile toolbox for PCR-based tagging of yeast genes: new fluorescent proteins, more markers and promoter substitution cassettes. *Yeast*, **21**, 947–962.
5. Frey,S., Pool,M. and Seedorf,M. (2001) Scp160p, an RNA-binding, polysome-associated protein, localizes to the endoplasmic reticulum of *Saccharomyces cerevisiae* in a microtubule-dependent manner. *J Biol Chem*, **276**, 15905–15912.
6. Anand,M., Chakraborty,K., Marton,M.J., Hinnebusch,A.G. and Kinzy,T.G. (2003) Functional interactions between yeast translation eukaryotic elongation factor (eEF) 1A and eEF3. *J Biol Chem*, **278**, 6985–6991.
7. Knop,M., Siegers,K., Pereira,G., Zachariae,W., Winsor,B., Nasmyth,K. and Schiebel,E. (1999) Epitope tagging of yeast genes using a PCR-based strategy: more tags and improved practical routines. *Yeast*, **15**, 963–972.
8. Ausubel,F.M., Brent,R., Kingston,R.E. and Moore,D.D. (2002) Short protocols in molecular biology: a compendium of methods from current protocols in molecular biology.
9. Sambrook,J., Fritsch,E.F. and Maniatis,T. (1989) Molecular cloning.
10. Mumberg,D., Müller,R. and Funk,M. (1994) Regulatable promoters of *Saccharomyces cerevisiae*: comparison of transcriptional activity and their use for heterologous expression. *Nucleic Acids Res*, **22**, 5767–5768.
11. Irizarry,R.A., Hobbs,B., Collin,F., Beazer-Barclay,Y.D., Antonellis,K.J., Scherf,U. and Speed,T.P. (2003) Exploration, normalization, and summaries of high density oligonucleotide array probe level data. *Biostatistics*, **4**, 249–264.